

Composite Coatings of Si₃N₄-Soda Lime Silica Produced by the Thermal Spray Process

A. Kucuk, R.S. Lima, and C.C. Berndt

(Submitted 3 August 2000)

Silicate glass and glass-silicon nitride composite coatings were atmospheric plasma sprayed onto mild carbon steel substrates under varying process parameters such as torch power and H₂/Ar ratios. The x-ray analysis revealed that Si₃N₄ in the composite coatings could be preserved under the harsh environmental conditions of the plasma spray process. The presence of Si₃N₄ as the reinforcement phase to the glass matrix conferred higher hardness properties to the coatings.

Keywords coatings, silicon nitride, soda glass, thermal spraying, parameter development, processing science

1. Introduction

Thermal spray technology has been widely used to produce ceramic, metal, cermet, and polymer coatings for various engineering applications such as insulative thermal barrier coatings, wear-resistant cermet coatings, and corrosion-protective metal and polymer coatings.^[1] The thermally sprayed coatings can be superior to their bulk counterpart since they provide the combined characteristics of two materials; *i.e.*, an underlying material (substrate) and the surface coating that is engineered for the operational environment. In yttria partially stabilized zirconia (YSZ) thermal barrier coatings on superalloy turbine blades, for instance, the ductile characteristics of a metal combine with refractory and corrosion resistance of the metal/ceramic coating. The attempt to use only one of the components (substrate or coating material) in this specific application fails. Many engineering ceramics, including oxides and carbides, have been sprayed for various engineering applications using thermal spray technologies such as plasma spray, high-velocity oxy-fuel spray and flame spray.^[2,3]

Silicate glasses have scientific and engineering applications that range from use as chemically durable containers to optical waveguides.^[4] Few silicate glass compositions have been reported as being thermally sprayed.^[5–9] However, their poor mechanical properties limit their applications. In the current study, a composite approach to producing glass coatings with improved mechanical properties was examined. Silicon nitride (Si₃N₄) was selected as the reinforcement constituent in the planned composite system. Silicon nitride is a ceramic with superior low- and high-temperature mechanical properties and chemical durability.^[10]

Thiel *et al.*^[11] attempted to spray Si₃N₄ thermally with the aid of binders such as silicon and amorphous alumina yttria. Echardt *et al.*^[12] followed a procedure in which Si₃N₄ was

reactive-plasma sprayed in a controlled nitrogen atmosphere using silicon powder. However, they found that Si₃N₄ suffers from decomposition under the harsh spray environment.

The current study aims to plasma spray glass coatings reinforced with Si₃N₄ to provide coatings with improved mechanical properties. This study also serves as a preliminary work toward spraying Si₃N₄-based materials with the aid of silicate glass as a binder.

2. Experimental Procedure

2.1 Feedstock Materials

Feedstock powders were (1) soda lime silicate (window glass and a mixture of Si₃N₄ (trial powder, Norton, Wochester, MA) and (2) window glass alone. Commercially available window glass with a typical composition of 14Na₂O-10CaO-3MgO-1Al₂O₃-72SiO₂ (wt.%) was crushed by quenching the glass plates heated to 700 °C in water and then ball milling with alumina media. The glass powder was dried at 120 °C and sieved to less than 105 μm prior to spraying. Composite feedstock powder was prepared by blending two volumes of window glass and one volume of Si₃N₄ powder for 1 h using a roller mixture and then by sieving to less than 105 μm. The mixture was dried at 120 °C and sieved again to <105 μm just prior to spraying.

2.2 Atmosphere Plasma Spraying

Feedstocks were atmosphere plasma sprayed on mild carbon steel substrates using a Metco 3MB torch with a Metco GH nozzle (Sulzer-Metco, Westbury, NY) mounted on a six-axis articulated robot traveling at a speed of 300 mm/s (model S400, GMF Fanuc, Charlottesville, VA). The spray parameters are listed in Table 1. The substrates of 25 × 25 mm dimensions were grit blasted to 4.5 ± 0.5 μm average roughness and cleaned with ethyl alcohol before spraying. External pressurized air was used to cool the samples from the front face during the spray process. The spray procedure was stopped after five passes for all coatings except for coatings FS-3 and FSA-3, which were sprayed as ten passes (Table 1).

Two coatings of each spray parameter were produced. One

A. Kucuk, R.S. Lima, and C.C. Berndt, Center for Thermal Spray Research, Department of Materials Science and Engineering, State University of New York at Stony Brook, Stony Brook, NY 11794-2275. Contact e-mail: cberndt@notes.cc.sunysb.edu.

Table 1 Spray conditions*

Parameters	F-1,	F-2,	F-3,	FS-1,	FS-2,	FS-3,
	FA-1	FA-2	FA-3	FSA-1	FSA-2	FSA-3
Current (A)	600	600	600	600	600	600
Voltage (V)	70	70	55	70	70	55
Primary gas, Ar (L/min)	40	50	50	40	50	50
Secondary gas, H ₂ (L/min)	12	10	9	12	10	9
Carrier gas, Ar (L/min)	5	5	5	5	5	5
Feed rate (rpm)	10	10	10	10	10	10
Stand-off distance (mm)	80	80	80	80	80	80
Thickness (μm/pass)	53	53	33	56	42	30

*One of each pair was annealed at 450 °C for 1 h and cooled in the furnace overnight. The “A” designator in the labels indicates samples that were annealed. The “F” and “FS” labels are for float (window) glass and float glass/Si₃N₄ composite coatings, respectively.

of these two coatings was annealed at 450 °C for 1 h and then cooled overnight in the furnace.

2.3 Characterization

The powder size distributions of the feedstocks were measured using a laser scattering particle size analyzer (Honeywell Inc., Minneapolis, MN).

The coatings were cut and polished for hardness measurements and microstructural analysis. A reflected light microscope (Nikon-Epiphot, Nikon Inc., Melville, NY) was used to examine the coating cross section. Some of the coating cross sections were also examined using a scanning electron microscope (ISI-SX-30, International Scientific Instruments, Santa Clara, CA).

Knoop hardness values of coatings on the cross-sectional areas were measured at 50 g load applied for 15 s using a Tukkon microhardness tester (Instron, Canton, MA).

The average roughness (*Ra*) of the coatings was measured using a Hommel T1000 mechanical profilometer (Hommel America, New Britain, CT). The roughness measurements were carried out with 0.5 mm/s traverse speed for a 15 mm length as described by the ISO 4287 standard procedure.^[13]

X-ray diffraction measurements were carried out on the feedstock powders and coatings using a computerized Philips PW 1729 x-ray diffractometer (Philips Electronic Instruments Corp., Mahwah, NJ) with Cu *K*_α radiation with 40 kV voltage and 30 mA current. The samples were scanned at a rate of 0.005°/s over a 2θ range of 20° to 60°.

3. Results

3.1 Particle Size Analysis

The glass and Si₃N₄ powders have similar particle size distributions (Fig. 1). The *d*₁₀, *d*₅₀, and *d*₉₀ were, respectively, 31, 83, and 132 μm for the sieved glass powder where *d*₁₀, *d*₅₀, and *d*₉₀ are the cumulative 10, 50, and 90% smaller particles, respectively. The *d*₁₀, *d*₅₀, and *d*₉₀ values were 53, 87, and 134 μm for the Si₃N₄ powder.

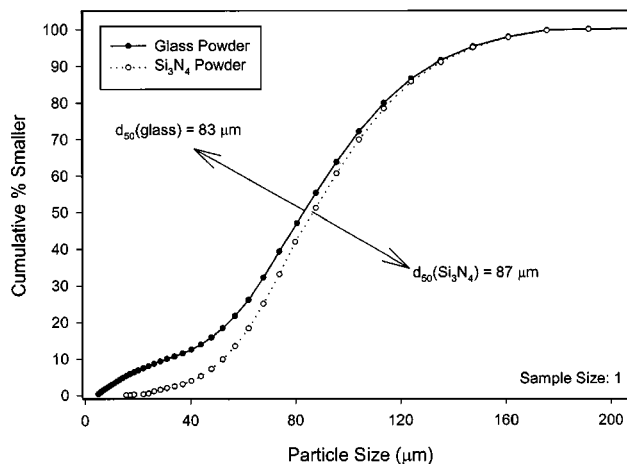


Fig. 1 Particle size distribution for glass and Si₃N₄ feedstock powders measured using laser scattering

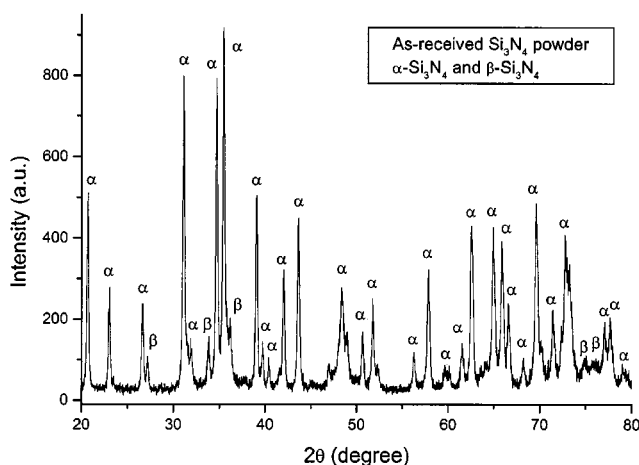
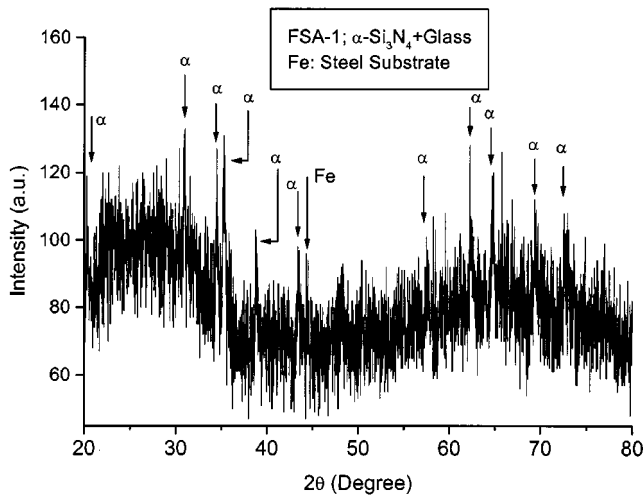


Fig. 2 X-ray diffraction pattern for as-received Si₃N₄ powder

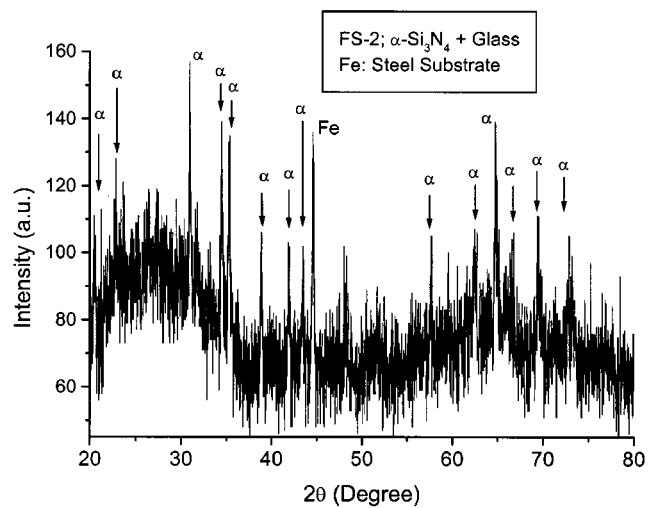
3.2 Phase Analysis

Figure 2 illustrates the x-ray diffraction pattern for as-received Si₃N₄ powder. As shown, the majority of powder is in α-Si₃N₄ form with a small amount of the high-temperature phase of β-Si₃N₄. JCPDS^[14] cards 9-250 and 9-259 were used to identify α-Si₃N₄ (hexagonal) and β-Si₃N₄ (hexagonal) phases, respectively.

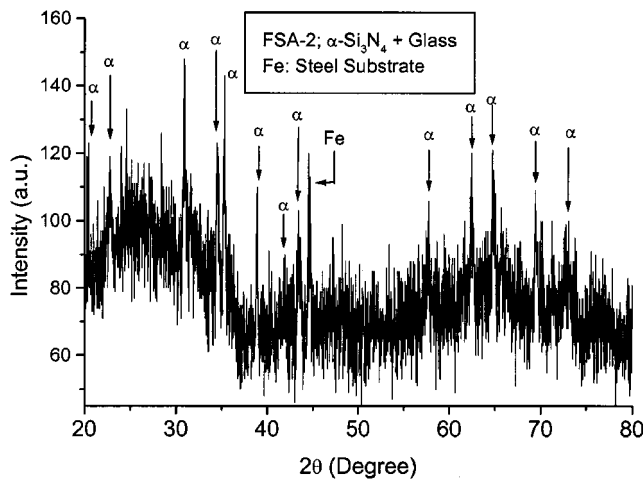
The x-ray diffraction patterns of Si₃N₄-glass composite coatings included an amorphous hump as well as sharp peaks for the crystalline phase (Fig. 3). The crystalline phase was identified as α-Si₃N₄. Some of the patterns included an iron peak that originated from the steel substrate. The intensity of α-Si₃N₄ peaks was much less than those of the powder due to the scattering resulting from the high surface roughness of the coatings and due to the presence of glass matrix around Si₃N₄. The intensity of α-Si₃N₄ peaks in the x-ray patterns obtained from coatings FS-2, FSA-2, and FSA-3 were slightly higher than that of FSA-1. No difference exists between the as-received (FS-2) and annealed (FSA-2) coatings sprayed under the same spray parameters (Table 1).



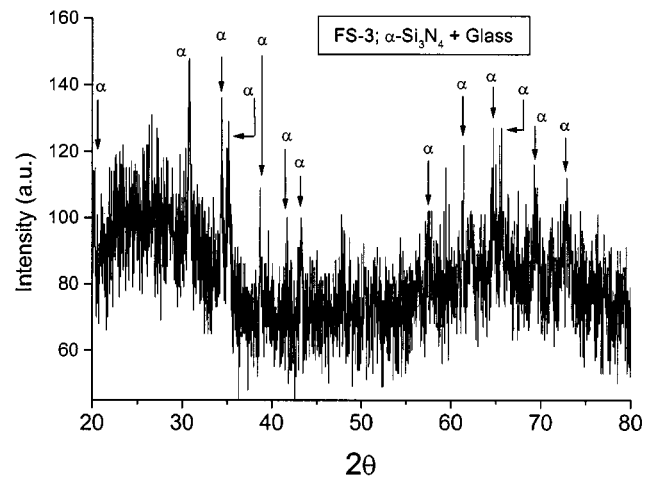
(a)



(b)



(c)



(d)

Fig. 3 X-ray diffraction pattern for glass/Si₃N₄ composite coatings: (a) sprayed with parameter 1 and then annealed, (b) sprayed with parameter 2, (c) sprayed with parameter 2 and then annealed, and (d) sprayed with parameter 3

3.3 Spray Capability of Feedstocks

Although the feedstock powder did not pass the Hall flow test (ASTM-B213),^[15] it was possible to inject it into the plasma jet at a constant rate using a mechanical injector. The thickness per pass for each coating sprayed as five or ten (for coatings FS-3 and FSA-3) passes is given in Table 1. The thicknesses of glass and composite coatings sprayed with the same parameters were similar. The spray parameter 1 provided coatings with higher thickness than parameters 2 and 3 (Table 1). The glass coatings were white/light gray in color and the composite coatings were dark gray.

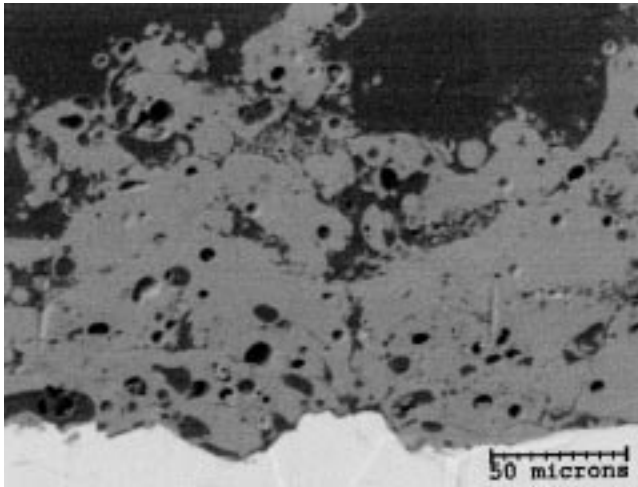
3.4 Microstructure

The typical images taken by scanning electron microscopy of the polished cross section of the coatings are presented in Fig. 4. In the micrographs, open and closed pores and pullouts from the polishing routine can be observed. The pullouts were

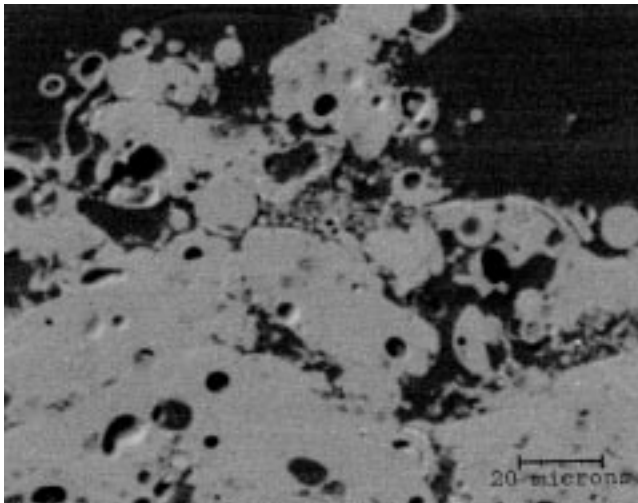
more obvious for coatings sprayed with parameter 3 than for parameter 1 and indicate that the cohesion between splats is weaker in these coatings. The closed circular pores evolve from gas trapped inside the glass drop and may arise from a change in the solubility of the dissolved gasses in glass with temperature^[16] or due to the entrapment of gasses during the spray process. The proportion of closed pores in the composite coatings was higher with respect to their glass counterpart due to the decomposition of Si₃N₄ to silicon and nitrogen.

3.5 Mechanical Properties

The Knoop hardness values measured on the cross section of the coatings along with the value for bulk glass and bulk Si₃N₄^[17] are presented in Fig. 5. The hardness of the coatings was lower by 25% than that of the bulk glass. The glass-Si₃N₄ composite coatings (designated as FS) exhibited higher hardness values than the glass coatings sprayed under the same



(a)



(b)

Fig. 4 Typical scanning electron microscopy images of a composite coating. Image in (b) is a closer view of the image in (a). In the images, the bright area is the substrate and the light and dark gray areas above the bright area are the coating and epoxy, respectively. Spherical closed pores and open pores (dark gray) can be seen throughout the coatings. Note that epoxy penetrated into the open pores

process conditions. Annealing of the coatings did not change the coating hardness.

Eversteijn *et al.*^[18] reported that annealed glasses exhibited higher hardness values compared to quenched glasses because quenched glasses have a more open structure (lower density) than the annealed glasses. Likewise, Hara and Kerkhof^[19] measured a Vickers hardness of 4% less with prestressed sheet glass than with annealed glass. Kranich and Scholze,^[20] using chemically hardened glasses, were able to show that the actual indentation is not changed through this strengthening or through the compressive stress associated with it. The elastic recovery, however, probably is increased. Therefore, one has to be cautious that quenched glasses have compressive stresses on the surface that would result in higher elastic recovery under indentation and give rise to a higher hardness reading.^[21] In general,

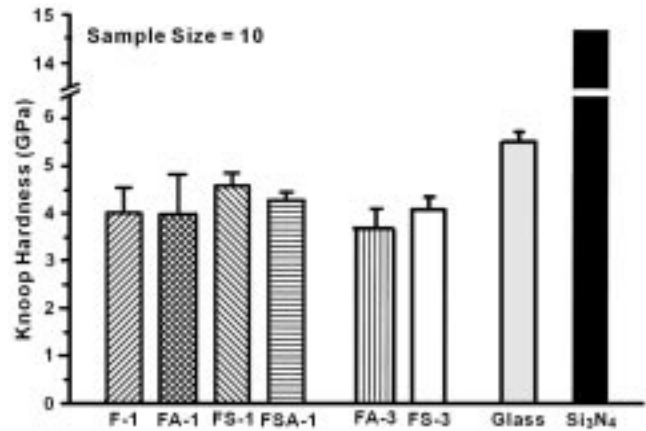


Fig. 5 Knoop hardness values measured on the cross-sectional area along with the values for float glass and Si₃N₄ bulk materials.^[17] Fifty grams of load was used for the measurements

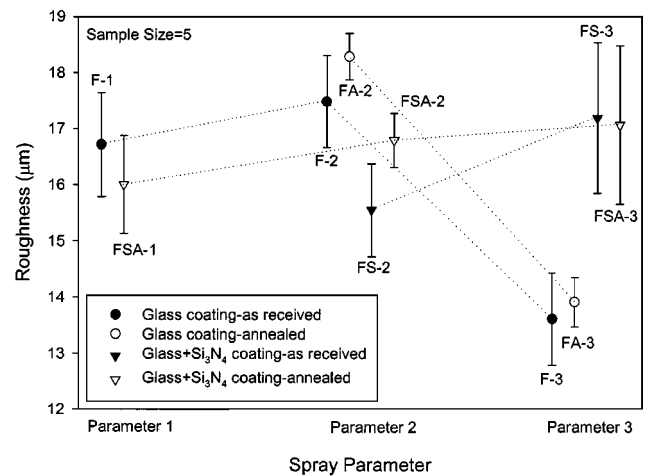


Fig. 6 Average roughness of coatings. Note that FA-1 and FS-1 were not available for roughness measurements

it is most probable to see no statistical difference between annealed and unannealed glasses if a simple hardness measurement procedure is applied.

There was no statistical difference between the hardness of either the glass or composite coatings sprayed under parameter 1 and parameter 3.

3.6 Roughness

The average roughness of coatings is presented in Fig. 6. The statistical analysis confirmed that annealing of coatings did not alter the coating roughness since the annealing temperature of 450 °C was too low for viscous flow, which could modify the microstructure. The roughness of glass coatings sprayed using parameters 1 and 2 was similar, whereas coatings sprayed with parameter 3 exhibited statistically significantly lower roughness than the aforementioned coatings. The Si₃N₄-glass composite coatings exhibited statistically similar

roughness values regardless of the spray parameters. The average roughness of the composite coatings sprayed using parameter 3 was statistically higher than the glass coatings sprayed with the same parameter.

4. Discussion

Although a coating thickness of 150 to 300 μm , which was thick enough for the applications, was obtained using the spray parameters given in Table 1, the deposition efficiency of the spray process was lower when compared to atmosphere plasma sprayed zirconia, which is a common plasma spray feedstock. Two hundred to five hundred micron thick YSZ coatings, for instance, were atmospheric plasma sprayed using hollow-sphere feedstock powder on mild carbon steel substrates using similar parameters with a 40 to 70% deposition efficiency;^[22,23,24] *i.e.*, 2 times thicker than the glass coatings. On the other hand, Sun *et al.*^[25] atmosphere plasma sprayed hydroxyapatite (HA) using the same spray conditions and they reported that 25 to 60 μm of HA deposits were generated per pass, which is similar to the deposition efficiency in the current work.

It was anticipated that hollow-sphere YSZ particles could totally melt depending on the temperature, whereas glass or HA particles could melt near the surface, but with an unmelted core. Therefore, the in-flight particle temperature and the percentage of molten/semimolten particles, which easily adhere on the substrate to form a deposit, are low during the spraying of glass. The average particle temperature for YSZ under similar plasma spray conditions, for instance, varied from 2100 to 2600 $^{\circ}\text{C}$ resulting in 10 to 35% molten/semimolten particles at the selected spray distances.^[22] It was expected that the average particle temperature for the glass particles was much lower. This fact can also be confirmed by the high roughness values observed in the coatings, which implies a low degree of melting.

The high roughness values observed in the range of 13 to 18 μm indicated that the spreading of splats upon impact was low. For example, the *Ra* values for thermally sprayed coatings such as YSZ,^[24] WC-Co,^[26] and HA^[27] coatings were reported as 5 to 10 μm . It was also reported that YSZ coatings have 50 to 300 μm diameter and 0.5 to 4 μm height cylinder-like splats.^[23,28,29] On the other hand, many spherical splats, which reflect poor spreading, can be observed in Fig. 4. In the plasma flame, glass particles were spheroidized, since this is the most thermodynamically stable balance between the surface tensile and bulk energy of a liquid.

As shown in Fig. 6, the *Ra* values of both glass and composite coatings were similar except for samples F-3 and FA-3 being slightly lower. The lower *Ra* for F-3 and FA-3 may arise because smaller particles adhered to the substrate to form the deposit. The average molten/semimolten particle size for YSZ in spray condition 1, for instance, was 50% larger than that in spray condition 3, bearing in mind that the torch power was 42 and 33 kW for conditions 1 and 3, respectively.^[22,23] Therefore, smaller glass particles that adhered to the substrate generated relatively lower roughness values.

As listed in Table 1, the thickness of the deposit produced per one pass using spray condition 1 was at least three times higher than that sprayed with condition 3 owing to the fact that torch power in condition 1 is 30% higher than that for condition

3. The glass and composite coatings were of similar thickness, indicating that Si_3N_4 was sprayed with a similar efficiency as the glass.

The x-ray patterns, color change, and hardness values confirmed the presence of Si_3N_4 in the composite coatings. As mentioned above, the intensity of the $\alpha\text{-Si}_3\text{N}_4$ peaks in the composite coating sprayed with condition 1 was slightly lower than the other two composite coatings (Fig. 3). This indicates that Si_3N_4 loss might be higher in condition 1 due to a relatively higher flame temperature. Nevertheless, the Si_3N_4 -reinforced coatings exhibited a 10 to 20% higher hardness (Fig. 5). It is believed that larger Si_3N_4 /glass ratios in the feedstock mixture would result in coatings with significantly enhanced mechanical properties.

5. Conclusions

Soda lime silicate (window) glass and glass/ Si_3N_4 composite coatings with 30 to 50 μm thickness were plasma sprayed. Higher plasma powers or higher H_2/Ar plasma gas mixture ratios produced thicker coatings since such conditions generated a plasma flame with higher temperatures.

X-ray analysis, hardness measurements, and visual inspections revealed that Si_3N_4 was deposited with glass without decomposing under the harsh plasma environment. The Si_3N_4 addition to glass, as reinforcement, improved the coating hardness. Further study needs to be carried out to investigate the influence of larger Si_3N_4 contents in the composite coatings.

The average roughness values of both glass and composite coatings were higher with respect to other plasma sprayed oxide coatings such as YSZ due to low heat exchange between the glass particles and the plasma flame.

Acknowledgments

Two authors (AK and CCB) acknowledge financial support from the National Science Foundation under NSF-MRSEC DNR, Grant No. 9632570. RSL acknowledges ONR Grant No. N00014-97-0843. Experimental assistance from Chris Dambra (under the URECA program), Matthew Gold, and Limin Sun, Materials Science and Engineering Department, State University of New York at Stony Brook, is appreciated.

References

1. L. Pawlowski: *The Science and Engineering of Thermal Spray Coating*, Wiley & Sons, New York, NY, 1995.
2. *Thermal Spray: A United Forum for Scientific and Technological Advances*, C.C. Berndt, ed., ASM International, Materials Park, OH, 1998.
3. *Thermal Spray: Surface Engineering via Applied Research*, C.C. Berndt, ed., ASM International, Materials Park, OH, 2000.
4. A.K. Vashneya: *Fundamentals of Inorganic Glass*, Academic Press, New York, NY, 1994.
5. P. Chraska, K. Neufuss, B. Kolman, and J. Dubsky: in *Thermal Spray: A United Forum for Scientific and Technological Advances*, C.C. Berndt, ed., ASM International, Materials Park, OH, 1998, pp. 477-81.
6. D.T. Gawne, Y. Bao, and T. Zhang: in *Thermal Spray: A United Forum for Scientific and Technological Advances*, C.C. Berndt, ed., ASM International, Materials Park, OH, 1998, pp. 467-72.
7. D.T. Gawne, Z. Qiu, T. Zhang, Y. Bao, and K. Zhang: in *Thermal*

- Spray: Surface Engineering via Applied Research*, C.C. Berndt, ed., ASM International, Materials Park, OH, 2000, pp. 977-81.
8. K. Neufuss, J. Ilavsky, J. Dubsky, B. Kolman, and P. Chraska: *United Thermal Spray Conf.*, E. Lugscheider and P.A. Kammer, eds., German Welding Society, Dusseldorf, 1999, pp. 636-40.
 9. T. Zhang, Z. Qiu, Y. Bao, D.T. Gawne, and K. Zhang: in *Thermal Spray: Surface Engineering via Applied Research*, C.C. Berndt, ed., ASM International, Materials Park, OH, 2000, pp. 355-61.
 10. F.L. Riley: *J. Am. Ceram. Soc.*, 2000, vol. 83 (2), pp. 245-65.
 11. S. Thiel, R.B. Heimann, M. Herrman, L.M. Berger, M. Nebelung, M. Zschunke, and B. Wielage: in *Thermal Spray: Practical Solutions for Engineering Problems*, C.C. Berndt, ed., ASM International, Materials Park, OH, 1996, pp. 325-31.
 12. T. Eckardt, W. Mallener, and D. Stover: in *Thermal Spray Industrial Applications*, C.C. Berndt and S. Sampath, eds., ASM International, Materials Park, OH, 1994, pp. 515-19.
 13. L. Mummery: *Surface Texture Analysis: The Handbook*, Hommelwerke, Muhlhausen, Germany, 1992.
 14. *Selected Powder Diffraction Data for Minerals*, 1st ed., Joint Committee on Powder Diffraction Standard (JCPDS), Philadelphia, PA, 1974.
 15. ASTM B213-90: Standard Test Method for Flow Rate of Metal Powders, *1994 Annual Book of ASTM Standards: Metallic and Inorganic Coatings; Metal Powder; Sintered P/M Structure*, ASTM, Philadelphia, PA, 1994, vol. 02.05, pp. 25-27.
 16. J.E. Shelby: *Handbook of Gas Diffusion in Solids and Melts*, ASM International, Materials Park, OH, 1996.
 17. A. Ezis and J.A. Rubin: *Engineering Materials Handbook: Ceramics and Glasses*, ASM International, Materials Park, OH, 1991, pp. 186-93.
 18. F.C. Everstejin, J.M. Stevels, and H.I. Waterman: *Phys. Chem. Glass*, 1960, vol. 1 (4), pp. 134-36.
 19. M. Hara and F. Kerkhof: *Rep. Asahi Glass Comp. Res. Lab.*, 1962, vol. 12, pp. 99-104.
 20. J.F. Kranich and H. Scholze: *Glastech. Ber.*, 1976, vol. 49, pp. 135-43.
 21. H. Scholze: *Glass: Nature, Structure, and Properties*, Springer-Verlag, New York, NY, 1991.
 22. A. Kucuk, R.S. Lima, and C.C. Berndt: *Am. Ceram. Soc.*, 2000, accepted for publication.
 23. A. Kucuk, R.S. Lima, and C.C. Berndt: *Am. Ceram. Soc.*, 2000, accepted for publication.
 24. R.S. Lima, A. Kucuk, and C.C. Berndt: in *Thermal Spray: Surface Engineering via Applied Research*, C.C. Berndt, ed., ASM International, Materials Park, OH, 2000, pp. 1201-05.
 25. L. Sun, C.C. Berndt, R.S. Lima, A. Kucuk, and K.A. Khor: in *Thermal Spray: Surface Engineering via Applied Research*, C.C. Berndt, ed., ASM International, Materials Park, OH, 2000, pp. 803-11.
 26. A. Kucuk: State University of New York at Stony Brook, Stony Brook, NY, unpublished work, 1999.
 27. C. Mancini, A. Kucuk, and C.C. Berndt: *J. Mater. Sci.*, 2000, submitted for publication.
 28. A.C. Leger, M. Vardelle, A. Vardelle, B. Dussoubs, and P. Fauchais: in *Thermal Spray Science and Technology*, C.C. Berndt and S. Sampath, eds., ASM International, Materials Park, OH, 1995, pp. 169-74.
 29. M. Vardelle, P. Fauchais, A. Vardelle, and A.C. Leger: in *Thermal Spray: A United Forum for Scientific and Technological Advances*, C.C. Berndt, ed., ASM International, Materials Park, OH, 1997, pp. 535-41.